Mutagenesis vol. 27 no. 6 pp. 653–663, 2012
Advance Access publication 27 July 2012
doi:10.1093/mutage/ges031

In vivo validation of DNA adduct formation by estragole in rats predicted by physiologically based biodynamic modelling

Alicia Paini[1,2,*], Ans Punt[1], Gabriele Scholz[2], Eric Gremaud[2], Bert Spenkelink[1], Gerrit Alink[1], Benoît Schilter[2], Peter J. van Bladeren[1,2] and Ivonne M.C.M. Rietjens[1]

[1]Division of Toxicology, Wageningen University, Tuinlaan 5, 6703 HE Wageningen, The Netherlands, [2] Nestlé Research Center, P.O. Box 44, Lausanne, Switzerland

*To whom correspondence should be addressed. Tel: + 0041 021 785 8701; Fax: + 0041 021 785 8553; Email: alicia.paini@wur.nl

Received on September 26, 2011; revised on April 13, 2012; accepted April 30, 2012

Estragole is a naturally occurring food-borne genotoxic compound found in a variety of food sources, including spices and herbs. This results in human exposure to estragole via the regular diet. The objective of this study was to quantify the dose-dependent estragole–DNA adduct formation in rat liver and the urinary excretion of 1'-hydroxyestragole glucuronide in order to validate our recently developed physiologically based biodynamic (PBBD) model. Groups of male outbred Sprague Dawley rats (*n* = 10, per group) were administered estragole once by oral gavage at dose levels of 0 (vehicle control), 5, 30, 75, 150, and 300 mg estragole/kg bw and sacrificed after 48 h. Liver, kidney and lungs were analysed for DNA adducts by LC-MS/MS. Results obtained revealed a dose-dependent increase in DNA adduct formation in the liver. In lungs and kidneys DNA adducts were detected at lower levels than in the liver confirming the occurrence of DNA adducts preferably in the target organ, the liver. The results obtained showed that the PBBD model predictions for both urinary excretion of 1'-hydroxyestragole glucuronide and the guanosine adduct formation in the liver were comparable within less than an order of magnitude to the values actually observed *in vivo*. The PBBD model was refined using liver zonation to investigate whether its predictive potential could be further improved. The results obtained provide the first data set available on estragole–DNA adduct formation in rats and confirm their occurrence in metabolically active tissues, i.e. liver, lung and kidney, while the significantly higher levels found in liver are in accordance with the liver as the target organ for carcinogenicity. This opens the way towards future modelling of dose-dependent estragole liver DNA adduct formation in human.

Introduction

The human diet is highly complex and a variety of naturally occurring genotoxic carcinogens can be found in food. One common mechanism and a presumed prerequisite for the carcinogenicity of most genotoxic compounds is the formation of DNA adducts (1). Analysis of DNA adducts has been used to complement data on carcinogen exposure, metabolism, mutation and tumour formation. The difficulties in assessing the risk of naturally occurring genotoxic carcinogens are well illustrated by the case of estragole. Estragole is present in spices and herbs such as basil, anise, fennel, bay leaves and tarragon, and in their essential oils and it is thus present in a variety of foods with a long history of human use, traditionally considered as safe. However, estragole is known to be hepatocarcinogenic at high doses in rodents (2). Estragole itself is not reactive but upon its rapid absorption in the gastrointestinal tract it is transported to the liver, where the compound is bioactivated (3). Metabolism of estragole can follow different pathways (Figure 1). Estragole is detoxified via *O*-demethylation to 4-allylphenol or epoxidation to estragole 2',3'-oxide and subsequent swift conversion of the epoxide by epoxide hydrolase and/or glutathione *S*-transferases (3,4). Estragole can also be converted to 3'-hydroxyanethole that can be glucuronidated and excreted in urine (5) or oxidised to 4-methoxycinnamic acid and in a follow-up step form 4-methoxybenzoic acid. The main pathway for bioactivation of estragole proceeds by initial hydroxylation on the allyl side chain by cytochrome P450 enzymes resulting in the formation of 1'-hydroxyestragole, the proximate carcinogenic metabolite. 1'-Hydroxyestragole can be detoxified by glucuronidation or via oxidation (4,6), the latter followed by glutathione conjugation. The glucuronidation of 1'-hydroxyestragole occurs in both humans and rats, being more dominant in rat than in human (7), whereas the oxidation of 1'-hydroxyestragole to 1'-oxoestragole has been demonstrated to represent a major pathway in humans but not in rats (7). Alternatively, sulfonation of 1'-hydroxyestragole by sulfotransferases gives rise to the unstable metabolite 1'-sulfooxyestragole that decomposes to generate the reactive carbocation that covalently binds to DNA, RNA and protein (4,8). Several adducts are formed upon reaction of 1'-sulfooxyestragole with the guanine base in DNA including N^2-(*trans*-isoestragol-3'-yl)-2'-deoxyguanosine, N^2-(estragole-1'-yl)-2'-deoxyguanosine, 7-(*trans*-isoestragol-3'-yl)-2'-guanine and 8-(*trans*-isoestragol-3'-yl)-2'-deoxyguanosine (4,9). The major guanine adduct formed is N^2-(*trans*-isoestragol-3'-yl)-2'-deoxyguanosine (E-3'-N^2-dGuo) (Figure 1) that is considered to play a role in the genotoxic and carcinogenic effects induced by estragole (3,4). The dG modifications have generally been reported as major adducts formed upon reaction of electrophiles with DNA because dG is the most potent nucleophilic nucleoside that can efficiently react with electrophiles (10,11). Recently it was reported that adducts between estragole and adenine may also be formed to a significant extent (12).

Several investigators have studied the mechanism of estragole carcinogenesis by examining DNA binding and characterising DNA adducts formed by estragole in mouse models. Randerath *et al.* (13) utilised ^{32}P-postlabelling to analyse DNA adduct formation in the livers of adult female CD-1 mice administered intraperitoneal (ip) injections of estragole, safrole and other alkenylbenzenes. Estragole and safrole exhibited the strongest

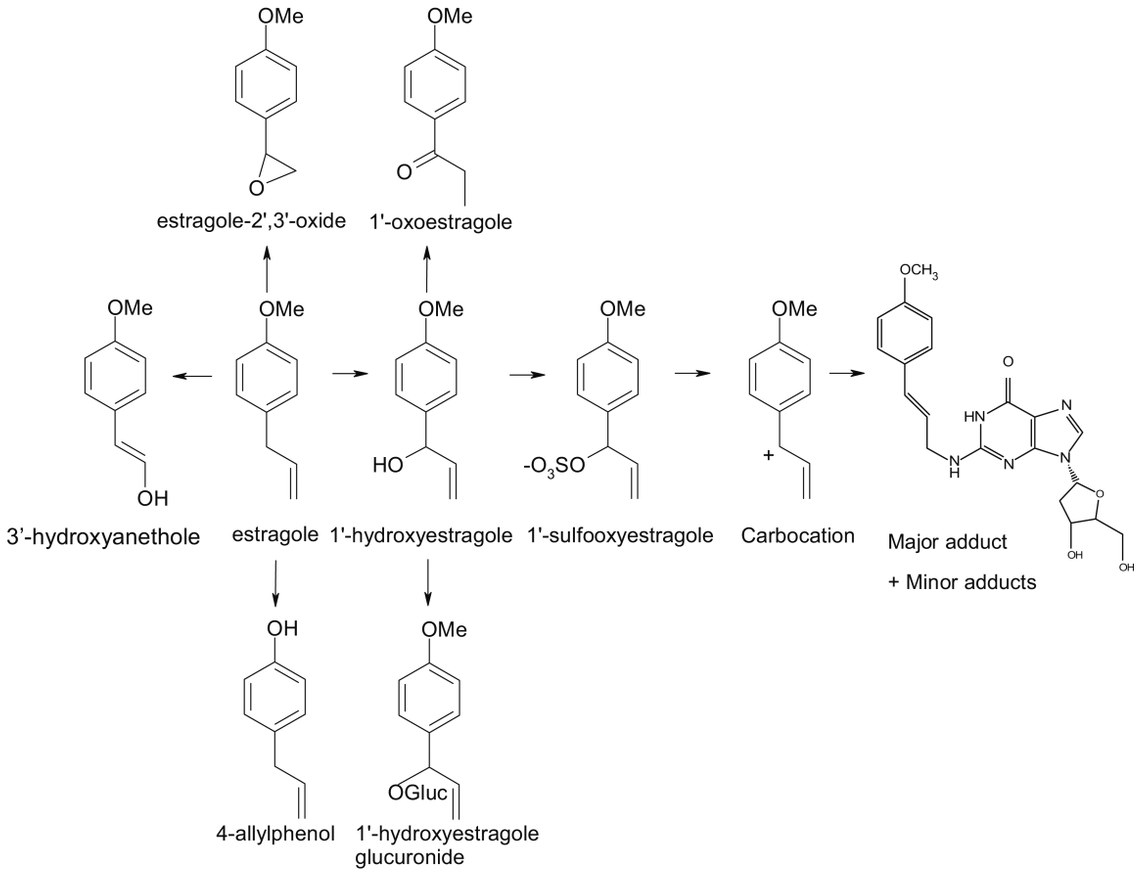

Fig. 1. Metabolism of estragole [adapted from Punt *et al*. (7)].

binding to mouse liver DNA (200–300 pmol adduct/mg DNA, at a 10-mg dose). Phillips *et al.* (14) found that estragole, methyleugenol and safrole formed adducts in liver DNA of newborn male B6C3F1 mice treated by ip injection on Day 1, 8, 15 and 22 after birth at doses of 0.25, 0.5, 1.0 and 3.0 µmol per animal. At Day 23 upon dosing the adduct levels with methyleugenol (72.7 pmol/mg DNA) were higher than those with estragole (30.0 pmol/mg DNA) and safrole (14.7 pmol/mg DNA) (14).

Recently, we defined a physiologically based biodynamic (PBBD) model to predict the dose-dependent DNA binding of estragole in rat liver (15) by extending the previously published physiologically based biokinetic (PBBK) model for rat (16). The PBBD model predicts the DNA adduct formation in the liver of rats at variable doses of estragole based on *in vitro* and *in silico* data only. However, the performance of the PBBD model developed could at the time not be evaluated due to the lack of *in vivo* data on DNA adduct formation in rats exposed to estragole. As detailed above, DNA adduct formation *in vivo* has to date only been studied in mice treated with estragole (13). Therefore, the objective of this study was to quantify the dose-dependent estragole–DNA adduct formation in rat liver and the urinary excretion of 1'-hydroxyestragole glucuronide in order to validate our PBBD model. The results obtained provide the first data set available on estragole–DNA adduct formation in rats and confirm DNA adduct formation in the metabolically active organs such as liver, lung and kidney, and also indicate that DNA adduct formation in the liver of estragole-exposed rats can be modelled within one order of magnitude accuracy using PBBD modelling.

Methods and materials

Materials

Estragole was obtained from Acros Organics (Geel, Belgium). 2'-Deoxyguanosine was purchased from Sigma (Basel, Switzerland). 1,2,3,7,9-$^{15}N_5$-2'-Deoxyguanosine ($^{15}N_5$-dGuo) was obtained from Cambridge Isotope Laboratories (Cambridge, MA). Alamethicin, β-glucuronidase, methanol, zinc sulphate (heptahydrate), phosphodiesterase I from Crotalus adamanteus (venom phosphodiesterase), phosphodiesterase II from bovine spleen (spleen phosphodiesterase), uridine 5'-diphospho-glucuronic acid (UDPGA) and alkaline phosphatase were purchased from Sigma (Schnelldorf, Germany). Acetonitrile, formic acid, dichloromethane, hydrochloric acid (37%), sodium carbonate, ammonium bicarbonate, sodium sulphate, petroleum ether, ethyl acetate, sodium acetate, tris(hydroxymethyl)aminomethane (Tris), ethylenediamine tetra acetic acid (EDTA), ammonia 30% and ethanol were purchased from Merck (Darmstadt, Germany). Nuclease P1 was obtained from MP Biochemicals (Aurora, OH). Triethylacetate ammonium buffer, acetic anhydride and pyridine were purchased from Fluka (Buchs, Switzerland) and β-glucuronidase was purchased from Roche (Mannheim, Germany). Heparin lithium tubes were purchased from Gosselin (Borre, France). Carboxymethyl cellulose (CMC; sodium salt, low viscosity—42.0 mPa s) was purchased from Calbiochem. Animal feed Teklad 2914C was purchased from Harlan Laboratories.

Synthesis of E-3'-N^2-deoxyguanosine (E-3'-N^2-dGuo) and ($^{15}N_5$) E-3'-N^2-deoxyguanosine [($^{15}N_5$) E-3'-N^2-dGuo] was carried out as reported in Paini *et al*. (15).

Determination of kinetic constants for glucuronidation of 1'-hydroxyestragole

Incubation with different batches of male Sprague Dawley rat liver S9 were performed to determine the Vmax and Km for glucuronidation of 1'-hydroxyestragole (OHES). Three batches were purchased from BD Bioscience (cat 452591 pooled Sprague Dawley rat liver S9—Batch 1: Lot 61642; Batch 2: Lot 74099; Batch 3: Lot 88875). The incubations were performed as previously described (16) using a final volume of 200 µl,

containing (final concentrations) 10 mM UDPGA and 0.2 mg/ml S9 protein in 0.2 M Tris–HCl (pH 7.4) containing 10 mM $MgCl_2$. The incubation mixture was pretreated on ice for 15 min with 0.025 mg/ml (final concentration) of alamethicin added from a 200 times concentrated stock solution in methanol (17,18). The incubation reactions were started after pre-incubation of 1 min by the addition of 1'-OHES at final concentrations varying from 50 to 2000 µM added from 200 times concentrated stock solutions in dimethylsulfoxide (DMSO). The incubations were carried out for 10 min at 37°C and terminated by adding 50 µl of cold acetonitrile. Blank incubations were performed without the cofactor UDPGA. 1'-Hydroxyestragole glucuronide was quantified by high-performance liquid chromatography (HPLC). Samples were centrifuged (16 000*g* for 5 min) and 50 µl of each supernatant were injected on an Alltima C18 5u column, 150×4.6 mm (Grace Alltech, Breda, The Netherlands) coupled to a HPLC-DAD system: a Waters 2695 Alliance system with a Waters 2996 photodiode array detector (Waters, Etten-Leur, The Netherlands). The gradient was made with ultrapure water containing 0.1% of acetic acid and acetonitrile. The flow rate was set at 1 ml/min and a linear gradient was applied from 10 to 25% of acetonitrile over 30 min, after which the percentage of acetonitrile was increased in 2 min to 100% and kept at 100% for 2 min. 1'-OHES glucuronide and 1'-OHES were quantified using a calibration curve of 1'-OHES recorded at a wavelength of 225 nm. For each batch Vmax and Km were determined in duplicate. The final Vmax and Km were calculated as the average of the three newly determined values and two data sets previously reported in the literature (16,19).

Physiologically based biodynamic modelling

The PBBD model was developed based on the PBBK model developed by Punt *et al.* (16) and described in detail previously (15) (Figure 2). As presented in the Results some PBBK model parameters were defined specifically for this study, including the parameters for body weight and organ weights that were based on the actual data obtained for the rats of this study. The kinetic parameters for glucuronidation of 1'-OHES were defined in more detail using different batches of liver microsomes. The kinetics of 1'-OHES glucuronidation appeared to have a major impact on the PBBK/BD model outcomes and previous studies revealed a significant variation for these kinetic parameters (7,16,19). Other parameters were kept similar to those reported and used before (7,19). It is important to note that the PBBD model is able to predict DNA adduct formation in the liver, the target organ, but not in kidney and lungs although these organs were included in the experimental analysis of DNA adduct formation *in vivo*.

To further improve the overall simulation of DNA adduct formation by the *in vitro* PBBD model, and to further reduce the differences between predicted and experimentally observed values, a refined PBBD model was defined taking two additional factors into account:

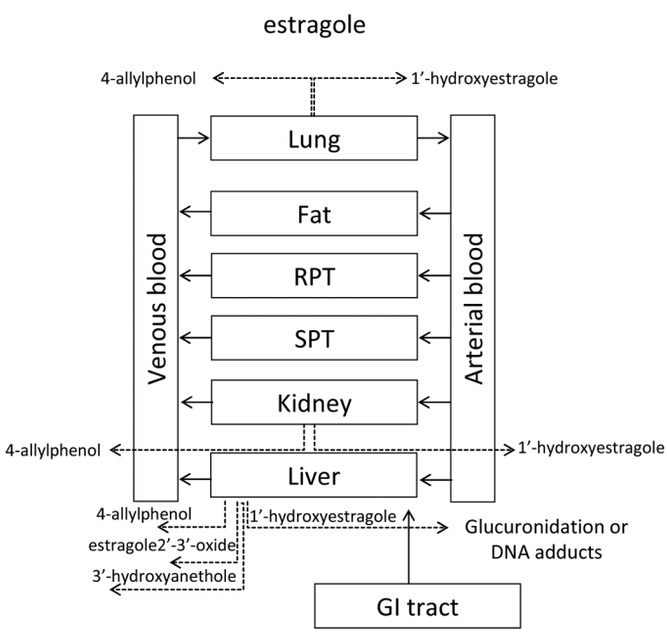

Fig. 2. Original schematic diagram of the proposed PBBK/BD model for estragole by Punt *et al.* (16).

1. Liver zonation dividing the liver compartment within the PBBD model into three equal zones: The liver architecture *in vivo* is not as homogenous as hepatocytes cultured *in vitro*. The heterogeneity of the liver implies that relevant biotransformation enzymes may be expressed in different parts of the organ to a different extent (20). The liver is mainly divided in a periportal zone (Zone 1), a mid-zone (Zone 2) and a perivenous zone (Zone 3). From the literature it can be derived that the enzymes involved in estragole hydroxylation in humans are CYP1A2, CYP2A6 and CYP2E1 (21). In rats, CYP2E1 and CYP1A2 are comparable to human CYP2E1 and CYP1A2, however, CYP2A6 in humans is comparable to CYP2A1/2 in rats (22). All these rat CYPs are more active in the perivenous zone of the liver as compared with the other zones (23). UDP glucuronosyltransferase (UGTs) are expressed in the perivenous zone (20,24) but also in the periportal zone (25,26). SULT enzymes are expressed preferentially in the periportal zone (20,24). To accommodate both possible locations of the UGTs two zonal models were described one with the UGTs in the perivenous zone (Zone 3) and another with the location of the UGTs in the periportal zone (Zone 1).
2. A submodel for 1'-OHES: Because the zonal models imply that upon its formation by CYPs in Zone 3 1'-OHES has to enter the systemic circulation before it can enter the liver in Zone 1 where sulfonation by SULTs or—in the second approach—glucuronidation by UGTs will take place, a submodel for the estragole metabolite 1'-OHES was added to the PBBD model, allowing the metabolite to enter the systemic circulation before its further conversion. Furthermore, given that systemic distribution of 1'-OHES will also provide possibilities for its conversion by extrahepatic metabolism we allowed—as a first approximation—only 60% of the 1'-OHES formed in Zone 3 to re-enter the liver. The value of 60% was based on the fact that the relative amount of DNA adduct formation in liver, lung and kidney indicated that at least for the SULT-mediated bioactivation of 1'-OHES ~60% occurred in the liver, the other part occurring in kidney (~5%) and lungs (~35%) (see Results).

The new PBBD model is graphically depicted in Figure 3. The Supplementary File, available at *Mutagenesis* Online presents the equations for this refined PBBD model.

Animals

The animal studies were in compliance with the Dutch Act on animal experimentation (Stb, 1977, 67; Stb 1996, 565), revised February 5, 1997. The study was approved by the ethical committee on animal experimentation of Wageningen University. All procedures were considered to avoid and minimise animal discomfort. Male Sprague Dawley rats, 6 weeks old, were purchased from Harlan laboratories (The Netherlands). Rats were housed in type IV cages with Lignocel bedding (Lignocel BK 8/15), accommodating three rats per cage. Enrichment was provided, i.e. paper tissue, for each cage. Animal cages were cleaned according to the standard protocols. A photoperiod of 12-h light/dark cycle for the rats was applied during the animal acclimatization period and treatment period. Temperature (21°C ± 1°C) and humidity (55 ± 10%) were monitored daily. Teklad 2914C pellet feed and tap water were provided *ad libitum* during the overall period of the study (from arrival at the facility to sacrifice).

Time-response study

The total number of animals for the time-response study was 25 white male outbred Sprague Dawley rats, 6 weeks old (174 g; SD ± 6). Upon arrival, animals were split randomly into cages and weighed 24 h after arrival at the facility, 7 days after arrival and 12 days after arrival. After a 12-day acclimatization period in type IV cages in groups of three animals per cage, animals were put into metabolic cages 24 h prior to gavage and were kept in the metabolic cages up to time of sacrifice. Animals were treated with a single dose of estragole of 300 mg/kg bw by gavage using a solution of estragole of 130 mg/ml in 0.5% CMC (0.5 g of CMC in 100 ml of distilled water), with the volume of gavage not exceeding 10 ml/kg. Animal average weight was 242.3 g (SD ± 9.5) at treatment and 241.3 g (SD ± 10.9) at sacrifice. After treatment animals were sacrificed at 2, 6, 24 or 48 h. For the 48-h time point a control was also introduced with five rats receiving only the vehicle control 0.5% CMC. Anaesthesia was done with a mixture of isoflurane and oxygen, blood was removed after which the liver was harvested, weighed and cut into pieces, snap frozen in liquid nitrogen and stored at −80°C until further processing.

Dose-response study

The total number of animals for the dose-response study was 60 white male outbred Sprague Dawley rats, 6 weeks old (177.1 g; SD ± 4.4). Upon arrival animals were split randomly into cages and weighted 24 h after arrival at the facility, 7 days after arrival and 12 days after arrival. After a 12-day

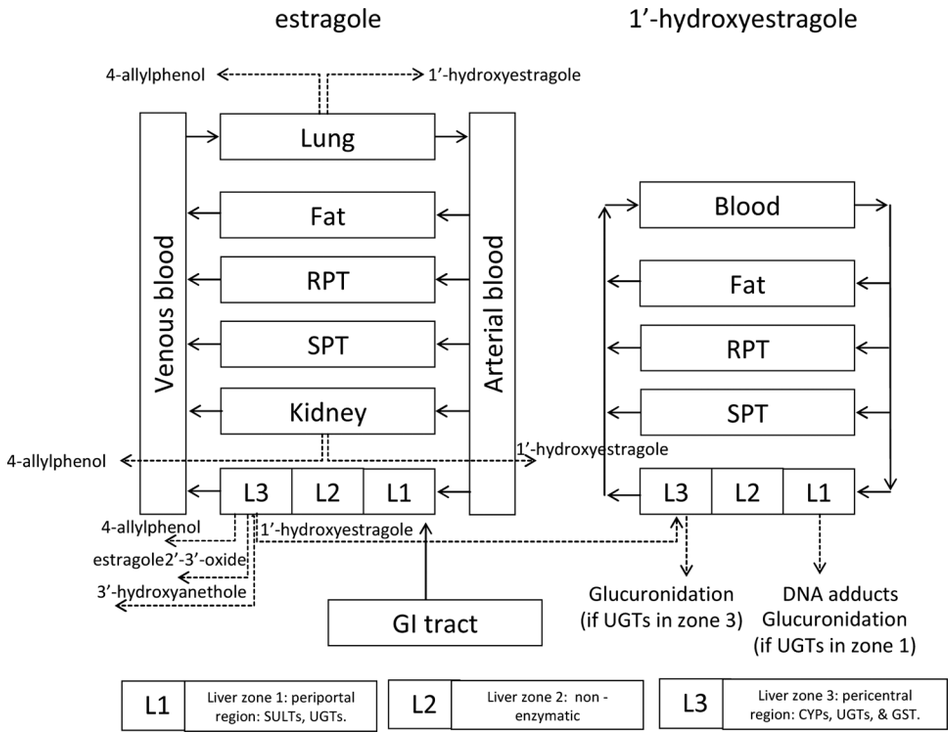

Fig. 3. Schematic diagram of the new proposed PBBK/BD model for estragole in rodents, with a 1'-OHES submodel and the liver compartment (L) subdivided into three equal zones: L1. A periportal zone containing the sulfotransferase (SULTs) activity and glucuronsyltransferases (UGTs). L2. A middle zone modelled without relevant enzyme activity. L3. A pericentral zone including the CYPs and glucuronsyltransferases (UGTs). GI, gastro intesintal tract; RPT, rapidly perfused tissue; SPT, slowly perfused tissue.

acclimatization period in type IV cages in groups of three animals per cage, animals were put into metabolic cages 24 h prior to gavage and were kept in the metabolic cages up to time of sacrifice. The following doses were administered once to the rats: 0 mg/kg bw (vehicle control 0.5% CMC), 5, 30, 75, 150 or 300 mg/kg bw of estragole using a solution of estragole of 2.5, 15, 37, 76 and 150 mg/ml in 0.5% CMC, respectively. The volume of gavage did not exceed 10 ml/kg. Urines were collected twice a day (morning and afternoon) and were stored at −80°C until further analysis. Rats were sacrificed after 48 h. Average weight at treatment was 255.3 g (SD ± 9.8) and at sacrifice it amounted to 263.0 g (SD ± 10.23). After anaesthesia of the animals with a mixture of isoflurane and oxygen, blood was removed and then liver, kidney and lungs were harvested, weighed and cut into pieces, snap frozen in liquid nitrogen and stored at −80°C until further processing. Blood was collected before removing organs in heparin tubes (4 ml), kept on ice and centrifuged (2000 rpm for 20 min, Sigma 2D centrifuge) and plasma was stored at −80°C in aliquots for further analysis.

Tissue DNA extraction and digestion

DNA was extracted from liver, kidney and lungs using the Get pure DNA Kit-Cell protocol (Dojindo Molecular Technology Inc., Kumamoto, Japan) for tissue (following the manufacturer's instructions). Briefly, three samples of each tissue were taken randomly from all organs, around 50–100 mg of each organ were put into a 2 ml eppendorf tube, and 800 µl of the lysis buffer with 20 µl of proteinase K solution were added. Homogenisation of tissue was done using a Fast Prep cell disruptor instrument. The homogenised samples were further processed following the manufacturer's protocol (Dojindo Molecular Technology Inc., Kumamoto, Japan). The final DNA pellet was dissolved in 100 µl MilliQ water. The yield and purity of the extracted DNA was determined using the Nanodrop technique by measuring the absorbance ratio A260 nm/A280 nm. DNA samples with an absorbance ratio of 1.8–2 were considered sufficiently pure. The quantity of DNA per sample was calculated from the Nanodrop output in ng/ml using a molar extinction coefficient for double-stranded DNA of 50 ($L \times mol^{-1}cm^{-1}$). The method of digestion was modified from Delatour *et al.* (27) for the release of the nucleosides E-3'-N^2-dGuo. Briefly, per 50 µg of DNA in 100 µl of water, 20 µl of buffer P1 (300-mM sodium acetate, 1-mM $ZnSO_4$, pH 5.3), 12 µl of spleen phosphodiesterase solution (0.0004 U/µl in water) and 10 µl of nuclease P1 (0.5 µg/µl in water) were added and the resulting solution was incubated for 4 h at 37°C. Following incubation, 20 µl of PA buffer (500 mM Tris–HCl, 1 mM EDTA, pH 8.0), 13 µl of venom phosphodiesterase solution (0.00026 U/µl in water) and 5 µl of alkaline phosphatase (0.764 U/µl in water) were added and the mixture was incubated for 3 h at 37°C (15,25). The hydrolysed sample was evaporated to dryness and reconstituted in 50 µl of water.

Isotope dilution quantification of E-3'-N^2-dGuo

Quantification of the nucleoside E-3'-N^2-dGuo by isotope dilution was done as reported in Paini *et al.* (15). Briefly, 50 µl of digested DNA from rat tissue were spiked with 10 µl of the internal standard ($^{15}N_5$) E-3'-N^2-dGuo to achieve 5 ng (0.012 nmol) injection of the internal standard into the instrument using an injection volume of 10 µl. In order to quantify the amount of adduct formed in the samples, a calibration curve was prepared using increasing concentrations of E-3'-N^2-dGuo with a constant concentration of ($^{15}N_5$) E-3'-N^2-dGuo.

LC–MS/MS method for detection and data analysis of E-3'-N^2-dGuo

LC–MS/MS analysis was performed on a Perkin Elmer 200 Series HPLC System (Perkin Elmer, Waltham, MA) coupled to a API 3000 system (Applied Biosystem, Foster City, CA). Samples were injected on an Agilent Zorbax Extend-C18 column, 2.1 × 50 mm, 3.5 Micron 80 Å (Basel, Switzerland), with a Zorbax guard column. The gradient was made with ultrapure water containing 0.1% (v/v) formic acid and 100% acetonitrile. The flow rate was set at 0.3 ml/min. A linear gradient was applied from 10 to 50% acetonitrile over 3 min, after which the percentage of acetonitrile was brought to 100% in 1 min, and kept at 100% acetonitrile over 2 min. The amount of acetonitrile was lowered to 10% over 1 min, and the column was equilibrated at these initial conditions for 8 min. E-3'-N^2-dGuo eluted at 2.88 min. The mass spectrometric analysis was performed with the following settings: Nebuliser gas (air) was set at 15 psi, Curtain gas (nitrogen, which is used to keep the analyser region clean) was set at 10 psi, ion spray voltage was 4700 V, collision energy (CE) was 15 eV, ion source temperature was set at 300°C, declustering potential was set at 37V, focusing potential was set at 200V, entrance potential at 9 V and collision cell exit was set at 12 V. Nitrogen was used as sheath gas turbo, ion spray, with a pressure of 7000 l/h. The dwell time per transition was 0.05 sec. A divert valve was used in order to discard the gradient after elution of the peak. Quantification of the DNA adduct was carried out using selected-ion detection in the multiple reaction-monitoring (MRM) mode, recording the following characteristic transitions—for the E-3'-N^2-dGuo: 414 m/z → 298 m/z (CE = 18 eV); 414 m/z → 164 m/z (CE = 37 eV); and 414 m/z → 147 m/z (CE = 40 eV); for the

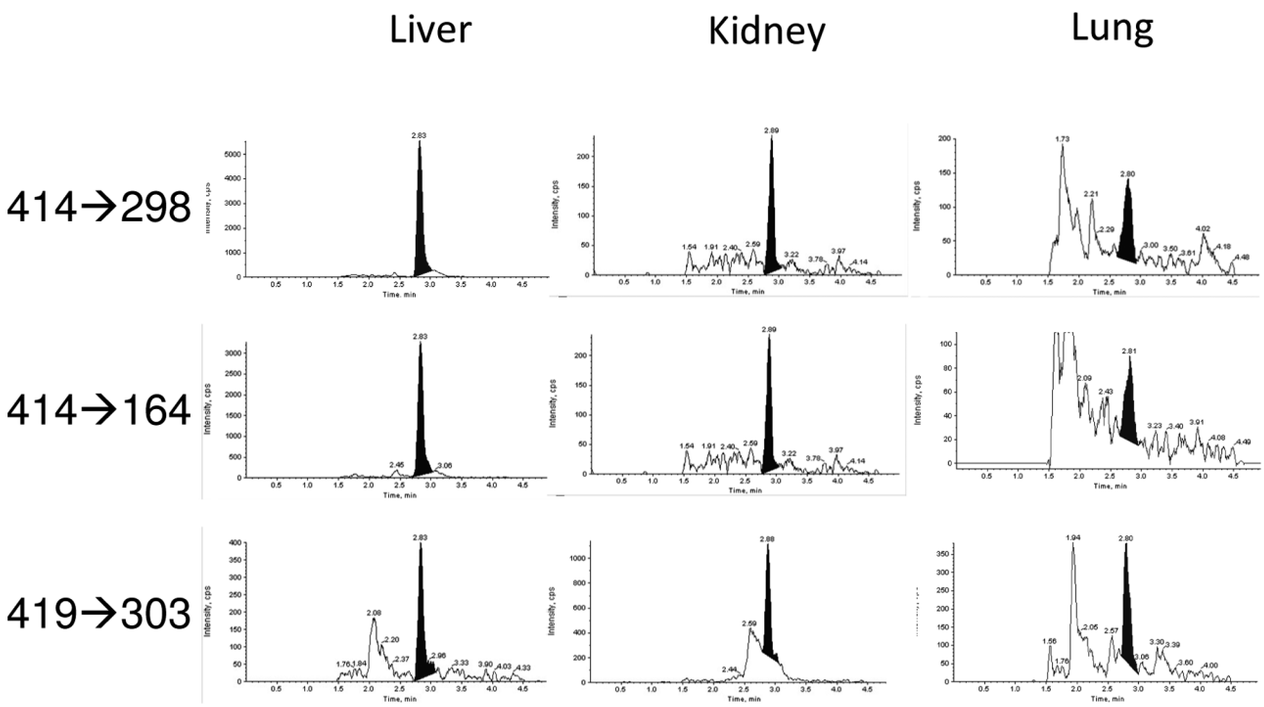

Fig. 4. Chromatograms representing the E-3'-N^2-dGuo adduct formed in liver, kidney and lungs at the quantifier transition (414 → 298), qualifier transition (414 → 164) and the peak of the internal standard ($^{15}N_5$) E-3'-N^2-dGuo (419 → 303). The highlighted peak reflects the presence of the adduct.

($^{15}N_5$) E-3'-N^2-dGuo: 419 m/z → 303 m/z (CE = 18 eV); 419 m/z → 169 m/z (CE = 37 eV). Figure 4 shows the chromatograms of the E-3'-N^2-dGuo (414 → 298, quantifier) adduct formed in the three organs 48 h after a dose of 300 mg/kg bw, along with the qualifier transition (414 → 164) and the peak of ($^{15}N_5$) E-3'-N^2-dGuo (419 → 303).

Data analysis of the calibration series and sample sequence was performed using Analyst software (Applied Biosystem) and integrated using an Excel spreadsheet developed internally (Nestlé Research Center), to comply with EU guidelines 2002/657/EC concerning the performance of analytical methods and the interpretation of results (EU guidelines: 2002/657/EC). The amount of E-3'-N^2-dGuo detected in the samples was related to the total amount of digested DNA detected in each sample and adjusted for the average molecular weight of DNA monophosphorylated nucleotides (nt) of 327 g/mol, in order to quantify the number of E-3'-N^2-dGuo adducts per 1000 nucleotides. For samples resulting in a negative value or below the Limit of Detection (LOD) a zero value was applied; and for samples resulting in a value below the Limit of Quantification (LOQ), the LOD value was applied.

Quantification of urinary excretion of 1'-hydroxyestragole glucuronide

Preparation and analysis of urines were done following the protocol reported by Zeller *et al*. (28). Urines were analysed, randomly for eight rats for each dose group. The vehicle control group was not analysed, since for each rat a urine sample was collected 24 h before treatment that served as control. Briefly, to 50µl urine sample 10 µl β-glucuronidase (0.36 U, 145 700 U/ml) in phosphate buffer (pH 5) were added. Samples were incubated at 37°C for 2 h. Subsequently the metabolites were extracted using 500 µl ethylether (twice), the sample thus obtained was centrifuged and transferred to a new Eppendorf tube, after which the sample was dried using a speed vacuum and reconstituted with 200 µl water. An isotope dilution technique was used to measure the amount of 1'-OHES released from 1'-OHES glucuronide compared with the internal standard D-1'-hydroxyestragole (26). D-1'-hydroxyestragole was prepared by AltanChim Pharma (Nantes, France). LC–MS/MS analysis was performed on a Perkin Elmer 200 Series HPLC System (Perkin Elmer, Waltham, MA) coupled with an API 3000 system (Applied Biosystem, Foster City, CA). Samples were injected on an Agilent Zorbax Extend-C18 column, 2.1 × 50 mm, 3.5 Micron 80 Å (Basel, Switzerland), with a Zorbax guard column. The gradient was made with ultrapure water containing 0.1% (v/v) formic acid and 100% acetonitrile. The flow rate was set at 0.3 ml/min. A linear gradient was applied from 10 to 50% acetonitrile over 3 min, after which the percentage of acetonitrile was brought to 100% in 1 min, and kept at 100% acetonitrile over 2 min. The amount of acetonitrile was lowered to 10% over 1 min, and the column was equilibrated at these initial conditions for 8 min. 1'-Hydroxyestragole eluted at 3.30 min. The mass spectrometric analysis was performed with the following settings: Nebuliser gas (air) was set at 15 psi, Curtain gas (nitrogen, which is used to keep the analyser region clean) was set at 12 psi, ion spray voltage of 2200 V, collision energy (CE) of 15 eV, ion source temperature at 300°C, declustering potential was set at 28 V, focusing potential was set at 200 V, entrance potential at 12 V and collision cell exit was set at 27 V. Nitrogen was used as sheath gas turbo, ion spray, with a pressure of 7000 l/h. The dwell time per transition was 0.05 sec. A divert valve was used in order to discard the gradient after elution of the peak. Quantification of the 1'-hydroxyestragole was carried out using selected-ion detection in MRM mode recording the following characteristic transitions—for 1'-hydroxyestragole: 147.2 m/z → 91.1 m/z (CE = 18 eV); 147.2 m/z → 115.1 m/z (CE = 37 eV); 147.2 m/z → 131.2 m/z (CE = 40 eV); for D-1'-hydroxyestragole: 150.2 m/z → 93.1 m/z (CE = 18 eV); 150.2 m/z → 118.1 m/z (CE = 37 eV); 150.2 m/z → 134.2 m/z (CE = 40 eV).

Statistical analysis

A *t*-test was performed using Excel (Microsoft Office 2010). Correlation analysis was performed using GraphPad Prism 5 (Version 5.04, 2010; GraphPad Software, Inc.). Vmax and Km were obtained using Graph pad Prism 5 (La Jolla, CA), by selecting XY analyses—nonlinear regression and fitting the data to the standard Michaelis–Menten equation.

Results

Refinement of the PBBD model

In order to validate the PBBD model the *in vivo* study was performed in two steps: first, a time-response study was carried out to determine the time point at which the level of DNA adducts in the target organ (liver) was maximal. Following this time-dependent study a dose-response study was performed using the time point determined in the first study, characterising the dose-dependent formation of DNA adducts in the liver and non-target organs (kidney and lungs) as well as the level of urinary excretion of 1'-OHES glucuronide.

Previously, we developed a PBBD model for estimation of *in vivo* estragole–DNA adduct formation based on experimental data on DNA adduct formation in primary hepatocytes (15).

Table I. Kinetic parameters for 1'-OHES glucuronide formation

Kinetic parameters	Punt *et al.* (7)	Al-husainy *et al.* (19)	Batch 1	Batch 2	Batch 3	Average	AverageAll
Vmax [nmol min^{-1} (mg S9 protein)$^{-1}$]	7.0	151	32.55	34.59	32.62	33.25	**51.5**
Km (µM)	137	241	201.2	211.1	226.7	209.5	**203.4**

Source: From References (7,19) and from experimental results using several batches of pooled male SD S9 fraction. The Vmax and Km values, average all, marked in bold were used for the simulation with the PBBD model.
Batches were purchased at BD Bioscience (cat 452591 pooled Sprague Dawley rat liver S9), for each batch the values are the average of two technical replicates. Batch 1: Lot 61642; Batch 2 : Lot 74099; Batch 3: Lot 88875.

This PBBD model allows estimation of the level of DNA adduct formation especially in rat liver after different doses of estragole. To make the PBBD model as accurate as possible some adjustments were made to the model previously described. These included first of all a precise definition of the body and organ weights taking into account the actual values of the male Sprague Dawley rats used in this study. Previously we applied as average body weight for male rats 250 g, and values for liver, kidney and lung weight of 8.5 g, 1.75 g and 1.25 g, respectively (15,16). In this study, the average body weight (for 60 animals) amounted to 263 g (SD ± 10.25) and the organ weights were 11.32 g (±0.75), 1.70 (±0.14) and 1.42 (±0.09) for liver, kidney and lung, respectively. Furthermore, the PBBD model published (15) was run for 2 h that was extended to 24 or 48 h, respectively, in this study in order to make a correct comparison with the *in vivo* experimental data, since 24 h was the time used for urine collection and 48 h was the time between dosing and sacrifice used in the *in vivo* DNA adduct dose-response study. The second improvement was that the kinetic parameters Km and Vmax for glucuronidation of 1'-OHES were quantified for different batches of liver microsomes (Table I). This was done because the sensitivity analysis of the model previously indicated these parameters to be of significant influence on the outcomes obtained (15), whereas they appeared to vary with the experimenter and with the batch of liver microsomes analysed (7,16,19) as shown in Table I. The average of five batches of male liver microsomes (three analysed and two obtained from the References 7,19) resulted in values for the kinetic parameters for glucuronidation of 1'-OHES that amounted to a Vmax of 51.5 nmol/min (SD ± 56) [(mg S9 protein)$^{-1}$] and a Km of 203.4 µM (SD ± 40) (Table I). These values were incorporated in the present PBBD model.

Time-dependent DNA adduct formation in vivo

Levels of DNA adducts in Sprague Dawley rats exposed by oral gavage to 300 mg/kg bw of estragole were measured in liver over time up to 48 h. Six random parts of each liver (50–100 mg) were used to extract the E-3'-N^2-dGuo adduct. The limit of detection of the adduct in the liver was 0.001 adduct/1000 nt (1 in 10^6 nt). Figure 5 shows the DNA adduct formation in liver over time after a dose of 300 mg/kg bw, which was found to be time dependent. The amount of adduct formed in the liver at 48 h was significantly higher (P = 0.003 by t-test) than the amount formed at 24 h. No adducts were detected in the control group, confirming that adduct formation is treatment related. Based on the results obtained 48 h post dosing was selected as the time point for analysis of DNA adduct formation in the subsequent dose-response study.

Dose-dependent DNA adduct formation in vivo

Levels of DNA adducts in male Sprague Dawley rats exposed once by oral gavage to increasing doses (0, 5, 30, 75, 150 and 300 mg/kg bw) of estragole were measured in liver, kidney and lungs 48 h after dosing (Figure 6). In the Supplementary File, available at *Mutagenesis* Online values for individual rats are reported, the results show for each dose group high variability between individuals. The limit of detection of the adduct was 0.001 adduct/1000 nt (1 in 10^6 nt) for liver and kidney, and 0.004 adduct/1000 nt (4 in 10^6 nt) for lung. In the liver a clear dose-dependent increase in E-3'-N^2-dGuo formation was found (Figure 6A). The level of DNA adducts detected 48 h after a dose of 300 mg/kg bw in this experiment can be compared with the value obtained in the time-response experiment. This revealed for the level of DNA adduct detected in the liver a somewhat higher amount of DNA adducts detected in the time-response experiment, amounting to 0.28 (SD ± 0.20) adducts/1000 nt (Figure 5) versus 0.10 (SD ± 0.08) adducts/1000 nt (Figure 6A) detected in the dose-response experiment, but the difference was not statistically significant. In lungs, DNA adducts were detected only at the two highest doses of estragole of 150 mg/kg bw and 300 mg/kg bw (Figure 6B). In kidney a dose response in DNA adduct formation was not observed, and levels were highest at the two highest dose levels (Figure 6C), with a statistically significant difference compared with the lower doses. At 300 mg/kg bw the amount of DNA adducts in the liver was 9 times higher than in kidney and 5 times higher than in lungs.

Comparison of the in vivo urinary excretion of 1'-hydroxyestragole glucuronide to the levels predicted by the PBBD model

Urine was collected in order to measure 1'-OHES glucuronide excretion and validate the outcomes of the PBBD

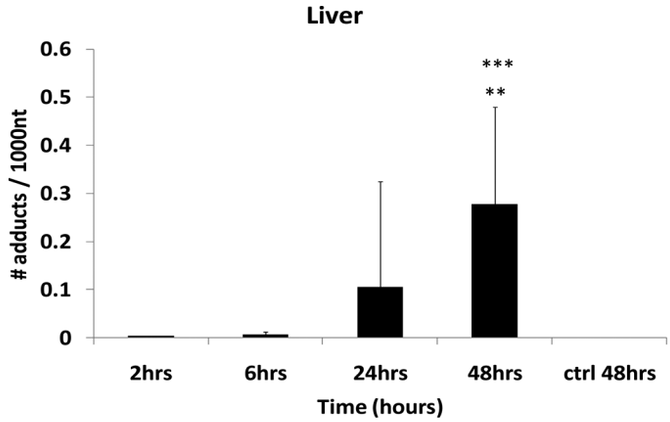

Fig. 5. Time-dependent DNA adduct formation in liver. DNA adducts are expressed as number of adducts in 1000 nt. A t-test was used to test for significant difference in maximal DNA adduct formation between 0 and 48 h (*** P <0.001) and between 24 and 48 h groups (** P <0.01); data represent the average and standard deviation of five rats, from which three technical replica were done.

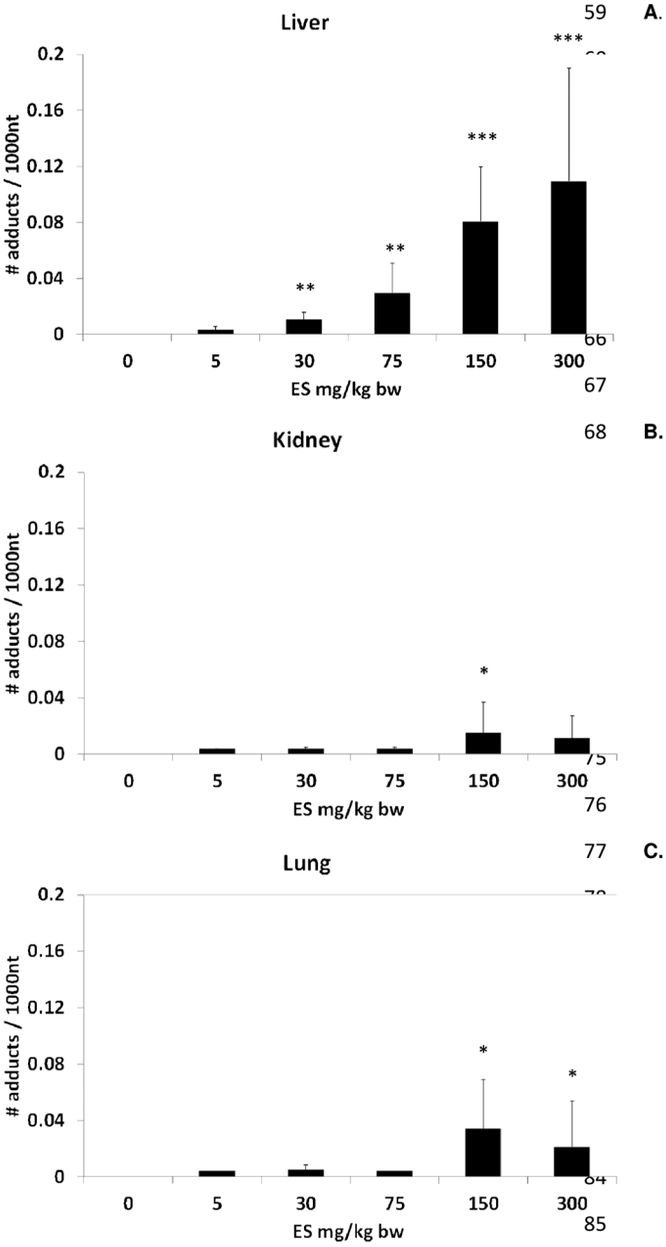

Fig. 6. Dose-dependent DNA adduct formation in liver (A), kidney (B) and lungs (C), DNA adducts are expressed as number of adducts in 1000 nt. A *t*-test was used to test for significant difference between treatment groups versus control group (*$P < 0.05$, **$P < 0.01$, ***$P < 0.001$); data represent the average and standard deviation of 10 rats, from which 3 technical replica were done.

model predicting the dose-dependent formation of this urinary metabolite. In the Supplementary File, available at *Mutagenesis* Online the urinary excretion of the 1'-OHES glucuronide measured for each dose group for eight individual rats from 0 to 24 h and from 0 to 48 h is reported. The results show for each dose group high variability between rats in excretion of the metabolite 1'-OHES glucuronide. Further, the results show a dose-dependent increase of 1'-OHES glucuronide in urine. For each dose the cumulative amount of 1'-OHES glucuronide formed was calculated by the PBBD model. Figure 7 shows the results obtained and also presents the data previously reported for urinary

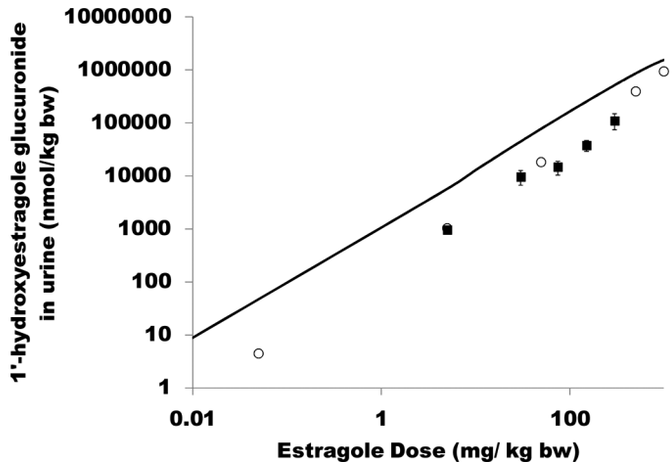

Fig. 7. PBBD model predicted (solid line) and experimentally determined 24 h urinary levels of 1'-OHES glucuronide at increasing oral doses of estragole. Data presented as black squares are the results of this study whereas those presented as open circles are those reported by Anthony *et al*. (5) for female Wistar albino rats. Data represent the average and standard deviation of eight rats.

excretion of 1'-OHES glucuronide by estragole-exposed female Wistar albino rats by Anthony *et al*. (5). The results obtained reveal that our data obtained for estragole-exposed male Sprague Dawley rats match those reported by Anthony *et al*. (5) for female Wistar albino rats. The results also reveal that the PBBD model–based predictions at 24 h upon dosing match the experimentally observed values within less than an order of magnitude since their predicted levels were 4.6–7.7-fold higher than the urinary levels actually observed.

Comparison of the in vivo results obtained to the levels of DNA adduct formation predicted by the PBBD model

Figure 8 presents a comparison between the dose-dependent formation of estragole–DNA adducts in the liver of male Sprague Dawley rats as experimentally determined in this study and as predicted by the PBBD model. The results reveal that the PBBD model–based predictions closely match the experimentally observed values. The PBBD model predictions at 48 h upon dosing appear to slightly overestimate DNA adduct formation by a factor of 1.9–2.3-fold.

Correlation of DNA adduct formation and the urinary biomarker 1'-hydroxyestragole-glucuronide

Figure 9 displays the relation between the number of DNA adducts formed (# adduct/1000nt) in liver and the amount of 1'-OHES (nmol/kg bw) excreted in urine as glucuronide conjugate. A significant positive correlation was found with increasing estragole dose between the number of DNA adducts and the concentration of 1'-OHES glucuronide in the urine after 48 h ($R^2 = 0.90$; Pearson coefficient p = 0.95; $P = 0.0118$; $n = 5$ data points each representing the average of eight rats).

Additional refinement of the PBBD model

To further improve the overall prediction of 1'-OHES glucuronide and DNA adduct formation by the model, a refined PBBD model was defined including division of the liver compartment in three equal zones (liver zonation) and the creation of a separate submodel for the estragole metabolite 1'-OHES,

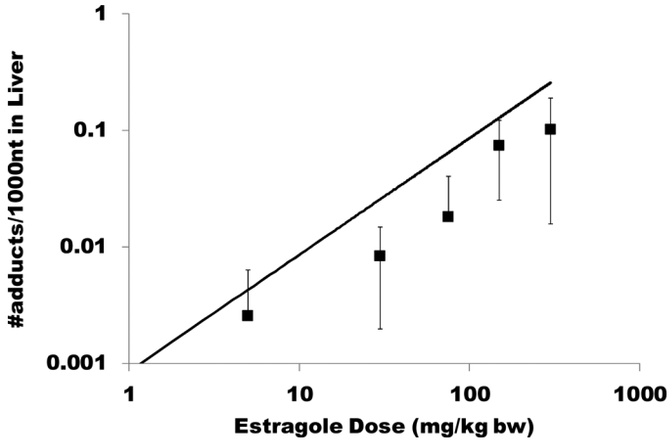

Fig. 8. *In vitro* PBBD model (solid line) prediction of the DNA adduct formation at 48 h versus DNA adducts measured *in vivo* (black square) at different oral doses of estragole. Data represent the average and standard deviation of 10 rats.

allowing only 60% of the 1'-OHES to re-enter the liver. This modification of the model reflects that the liver architecture *in vivo* is not homogenous; furthermore extrahepatic circulation of 1'-OHES may increase the chances on its conversion by extrahepatic enzymes reducing the chances on its conversion to a DNA reactive metabolite in the liver. Figure 3 presents a schematic overview of the refined model. The liver was described as three equal zones as explained in Manning *et al.* (20), where each zone differs in the overall expression of the enzymes involved in the metabolism of estragole and 1'-OHES. The activity of each enzyme was confined to only the specific zone where it is most highly expressed, with exception of the UGTs that were modelled in either Zone 1 or Zone 3. Figure 10A and 10B present the results obtained with the two new zonal models as compared with the predictions based on the original model and the experimental data. The results presented for DNA adduct formation in Figure 10A reveal that the predictions obtained using the refined model with the liver zonation and the submodel for 1'-OHES with glucuronidation in Zone 3 results in predictions that match the *in vivo* experimental values even better than the original

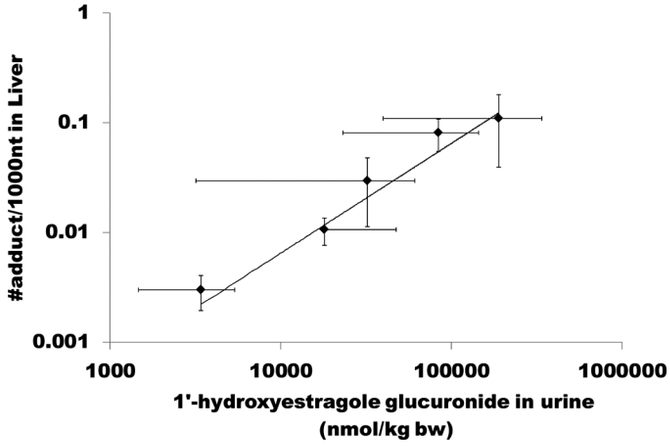

Fig. 9. Correlation between 1'-OHES glucuronide urinary excretion and estragole DNA adducts in the liver at increasing estragole doses ($R^2 = 0.90$; Pearson coefficient p = 0.95; $P = 0.0118$; $n = 5$ data points each representing the average of eight rats).

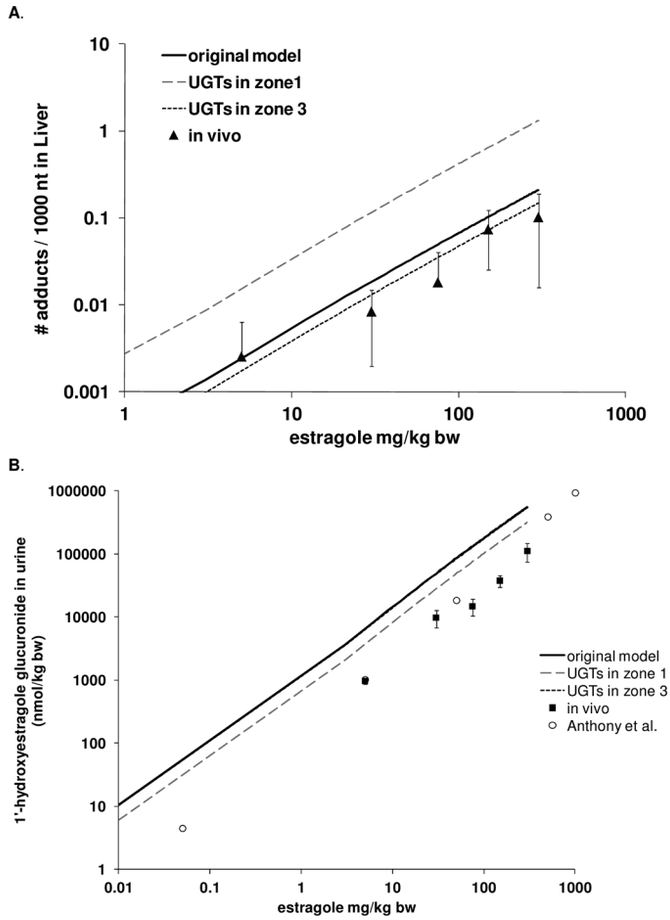

Fig. 10. (A) Comparison of experimental data obtained in this study for DNA adduct formation in the liver to their PBBK/PBBD–based predicted values when using either the original model (black lines) or the newly defined extended PBBK/PBBD models including liver zonation and a submodel for 1'-hydroxyestragole; (dashed lines). The two zonal models include UGTs in either Zone 3 (dashed black line) or Zone 1 (dashed grey line) and *in vivo* experimental data are presented as black triangles and represent the average and standard deviation of 10 rats. (B) Comparison of experimental data obtained in this study for formation of urinary 1'-hydroxyestragole glucuronide to their PBBK/PBBD–based predicted values when using either the original model (black lines) or the newly defined extended PBBK/PBBD models including liver zonation and a submodel for 1'-hydroxyestragole; (dashed lines). The two zonal models include UGTs in either Zone 3 (dashed black line) or Zone 1 (dashed grey line). Data presented as black squares are the results of this study whereas those presented as open circles are those reported by Anthony *et al.* (5) for female Wistar Albino rats. Urinary data (black squares) represent the average and standard deviation of eight rats.

model (Figure 10A, black dashed line). For the glucuronidation a slight improvement occurred compared with the original model (in Figure 10B the two lines coincide) and predicted data were generally 4–6-fold different from the experimental data (Figure 10B, black dashed line). In a second approach glucuronidation was modelled in Zone 1. The predicted DNA adduct formation matched the experimental data to a lower extent was 11-fold overpredicted (Figure 10A, grey dashed line; note the *y*-axis is a log scale). However, for the formation of 1'-OHES glucuronide predicted values matched the experimental data to a better extent with the deviation between predicted and experimental values being on average 2.8–5-fold (Figure 10B, grey dashed line).

It is important to note as well that in the refined models the full conversion of estragole takes more time reflected by a

continued increase in the amount of DNA adduct formation up to at least 30 h upon dosing 300 mg estragole/kg bw, which was 20 h in the original model without liver zonation.

Discussion

The aim of this study was to quantify dose-dependent estragole–DNA adduct formation in male Sprague Dawley rat liver and the levels of urinary excretion of 1'-hydroxyestragole glucuronide in order to validate the *in vitro* PBBD model previously built (15). The adduct measured and predicted in this was E-3'-N^2-dGuo, which was previously reported to be the most abundant adduct formed by estragole (10,11). Recently it was reported that adducts between estragole and adenine may also be formed to a significant extent (12). However, the formation of additional adducts to the E-3'-N^2-dGuo taken into account in this study will not affect the outcomes of this study since our measurements and the PBBD predictions focused on formation of E-3'-N^2-dGuo only within the liver.

The first validation step of the PBBD model in this study was based on the dose-dependent urinary excretion of 1'-OHES glucuronide. The results acquired reveal that our data obtained for estragole-exposed male Sprague Dawley rats match those reported by Anthony *et al*. (5) for female Wistar albino rats. The results also reveal that the PBBD model–based predictions match the experimentally observed values within less than an order of magnitude. Differences between the present data and those reported by Anthony *et al*. (5) may be caused by differences in the animal strain and sex. Animals used in Anthony *et al*. (5) study were female Wistar albino rats and those in this study male outbred Sprague Dawley rats. The PBBD model predicted somewhat higher levels of the 1'-OHES glucuronide compared with *in vivo* data, which was also found previously by Punt *et al*. (16), but deviations were generally within one order of magnitude. Given this result it is important to stress that deviations within one order of magnitude are generally considered acceptable within the present state-of-the-art of PBBK modelling (29). One explanation for the deviation in predicted urinary levels of 1'-OHES glucuronide could be that the actual bioavailability of estragole is lower than 100%. Another reason could be that in the present PBBK model excretion and further extrahepatic metabolism of 1'-OHES are not included, which may result in some overestimation of the levels of 1'-OHES in the liver and thus of 1'-OHES glucuronide and 1'-sulfooxyestragole predicted to be formed, and subsequently of the predicted urinary levels of 1'-OHES glucuronide and DNA adducts formed. The match between experimentally observed and predicted values is also considered adequate when it is taken into consideration that the current PBBD model was based on *in vitro* data only, whereas most current physiologically based kinetic or dynamic models use *in vivo* data to optimise parameters in the model and improve the fit (30 and references therein). The PBBD predictions were obtained using data from primary hepatocytes exposed to 1'-OHES and this implies that the level of DNA adduct formation implicitly includes the balance between DNA adduct formation and DNA repair (15). DNA adducts are known to be a biomarker of genotoxic exposure and urinary excretion of metabolites are biomarkers of early biological effect (31). Thus, a comparison between the experimental data for cumulative urinary excretion of 1'-OHES glucuronide and DNA adduct formation in the liver was made revealing a positive correlation. This suggests that with increasing dose of estragole a proportional increase in bioactivation occurs in the liver, which is reflected by an increased level of urinary excretion of 1'-OHES glucuronide. In the second step, the PBBD model–based predictions for formation of estragole–DNA adducts in the liver of male rats were compared with the experimental data obtained. Using the optimised new parameters the PBBD model–based predictions for the levels of adduct formation were within the same order of magnitude as the *in vivo* measurements. Data on DNA adduct levels in rats exposed to estragole have not been reported before. Thus the results of this study can only be compared with data obtained in estragole-exposed mice. Randerath *et al*. (13) reported in female CD-1 mice the formation of 1 adduct in 10 000–15 000 DNA nucleotides after a single ip injection of 10 mg estragole per mouse. Assuming a mouse weight of 0.025 kg, the dose was estimated to be 400 mg/kg bw. At our highest dose tested *in vivo* (300 mg/kg bw) we obtained 1 adduct in 10 000 nucleotides that is comparable with the value reported by Randerath *et al*. (13) although this value was obtained using a different technique for quantification of the DNA adduct levels, in a different species and at a different dose level. The amount of E-3'-N^2-dGuo adducts at a daily human exposure level of 0.01 mg/kg bw/day (3) and 0.07 mg/kg bw/day estragole (32), was predicted to be 0.44 and 3.1, respectively, in 10^8 nt. These levels of adducts are orders of magnitude below the background level of DNA damage of 100 adduct in 10^8 nt, which have been suggested to be of no known consequence (33).

To further improve the PBBD-based predictions a refined PBBD model was developed. This was done by dividing the liver compartment in three equal zones (20), where Zone 1 was assumed to contain sulfotransferase (SULT) activity and Zone 3 cytochrome P450 (CYP). The UGT enzymes were placed either in Zone 3 or in Zone 1, resulting in two zonal models. Furthermore, the refined models also included a submodel for 1'-OHES, to allow for its entering the systemic circulation, and only 60% was allowed back into the liver. This approach can be seen as a 'dilution factor' in time of the metabolite within the body increasing the time needed in the model for full conversion of the parent compound. From the results obtained it follows that the changes made within the model resulted in a somewhat better fit between the predicted and observed data with the improvements depending on the assumptions made about zonation of the UGTs. In addition it is important to note that when extrahepatic metabolism of 1'-OHES would result in a substantial formation of 1'-OHES glucuronide the level of this urinary metabolite predicted by the zonal models will be underestimated. The remaining discrepancy in predicted and observed levels of urinary 1'-OHES glucuronide might then rather be ascribed to other factors such as formation of other—as yet unidentified—metabolites of 1'-OHES reducing the amount that can be converted to the glucuronide conjugate. Additionally it may be due to chemical instability of the 1'-OHES (glucuronide) resulting in its isomerisation to 3'-hydroxyanethole leading to underestimation of the levels of 1'-OHES (glucuronide) in the urinary samples, or to reduced bioavailability of estragole assumed in the present model to be 100%. In order to understand this discrepancy further studies should be performed that were however beyond the scope of this study.

Furthermore, it is of interest to note that this study shows formation of DNA adducts not only in the liver, but also in the kidney and lung of male Sprague Dawley rats treated with estragole. These data could however not be compared with predicted values because the PBBD model did not include equations to predict DNA adduct formation in extrahepatic tissues.

The lower amount of DNA adducts detected in these organs reflects the low metabolic conversion of estragole to 1'-OHES found in these organs by Punt *et al*. (16), although the data indicate that these organs do contain the relevant cytochromes P450 and conjugating enzymes needed for bioactivation of estragole to some extent. To the best of our knowledge this is the first time DNA adducts were detected in liver, lung and kidney of estragole-treated rats. Interestingly, DNA adducts were detected *in vivo* in all three organs, but the metabolic capacity for DNA adduct formation and repair in lung and kidney is probably unevenly distributed over the different cell types in these tissues. This hampers their comparison with the data obtained for the liver, the target organ for estragole-induced tumour formation, where DNA adduct formation may be more evenly distributed.

In conclusion this study reveals a dose-dependent increase in estragole–guanine DNA adduct formation in the liver of rats exposed to estragole, and also corroborates that the now optimised PBBD model can provide a tool to examine dose-dependent DNA adduct formation in the liver of rats exposed to estragole. Extending this rat PBBD model to the human situation will provide a way to extrapolate from rats to the human situation including extrapolation from the high-dose rat experimental dose levels to low dose levels that are more realistic for human exposure regimens. This will provide further insight in species and dose-dependent differences or similarities in DNA adduct formation in the liver upon exposure to estragole.

Funding

Nestlé Research Center

Supplementary data

Supplementary files are available at *Mutagenesis* Online.

Acknowledegments

The authors gratefully acknowledge the excellent assistance from the co-workers of the center of laboratory animals (CKP) of Wageningen University (Wageningen, the Netherlands) during the *in vivo* part of this work.

Conflict of interest statement: None declared.

References

1. Preston, R. J. and Williams, G. M. (2005) DNA-reactive carcinogens: mode of action and human cancer hazard. *Crit. Rev. Toxicol.,* **35,** 673–683.
2. Miller, E. C., Swanson, A. B., Phillips, D. H., Fletcher, T. L., Liem, A. and Miller, J. A. (1983) Structure–activity studies of the carcinogenicities in the mouse and rat of some naturally occurring and synthetic alkenylbenzene derivatives related to safrole and estragole. *Cancer Res.,* **43,** 1124–1134.
3. Smith, R. L., Adams, T. B., Doull, J. *et al.* (2002) Safety assessment of allylalkoxybenzene derivatives used as flavouring substances—methyl eugenol and estragole. *Food Chem. Toxicol.,* **40,** 851–870.
4. Phillips, D. H., Miller, J. A., Miller E. C. and Adams, B. (1981) Structures of the DNA adducts formed in mouse liver after administration of the proximate hepatocarcinogen 1'-hydroxyestragole. *Cancer Res.,* **41,** 176–186.
5. Anthony, A., Caldwell, J., Hutt, A. J. and Smith, R. L. (1987) Metabolism of estragole in rat and mouse and influence of dose size on excretion of the proximate carcinogen 1′-hydroxyestragole. *Food Chem. Toxicol.,* **25,** 799–806.
6. Iyer, L. V., Ho, M. N., Shinn, W. M., Bradford, W. W., Tanga, M. J., Nath, S. S. and Green, C. E. (2003) Glucuronidation of 1'-hydroxyestragole (1'-HE) by human UDP-glucuronosyltransferases UGT2B7 and UGT1A9. *Toxicol. Sci.,* **73,** 36–43.
7. Punt, A. Paini, A., Boersma, M. G., Freidig, A. P., Delatour, T., Scholz, G., Schilter, B., van Bladeren P.J. and Rietjens I. M. C. M. (2009) Use of physiologically based biokinetic (PBBK) modeling to study estragole bioactivation and detoxification in humans as compared to male rats. *Toxicol. Sci.,* **110,** 255–269.
8. Gardner, I., Bergin, P., Stening, P., Kenna, J. G. Caldwell, J. (1996) Immunochemical detection of covalently modified protein adducts in livers of rats treated with methyleugenol. *Crit. Rev. Toxicol.,* **9,** 713–721.
9. Punt, A., Delatour, T., Scholz, G., Schilter, B., Van Bladeren, P. J. and Rietjens, I. M. C. M. (2007) Tandem mass spectrometry analysis of N2-(trans-isoestragol-3'-yl)-2'-deoxyguanosine as a strategy to study species differences in sulfotransferase conversion of the proximate carcinogen 1'-hydroxyestragole. *Chem. Res. Toxicol.,* **20,** 991–998.
10. Singh, R., Gaskell, M., Le Pla, R. C. *et al.* (2006) Detection and quantification of benzo[a]pyrene-derived DNA adducts in mouse liver by liquid chromatography-tandem mass spectrometry: comparison with 32P-postlabeling. *Chem. Res. Toxicol.,* **19**, 868–878.
11. Pfau, W., Brockstedt, U., Söhren, K. D. and Marquardt, H. (1994) 32P-postlabelling analysis of DNA adducts formed by food derived heterocyclic amines: evidence for incomplete hydrolysis and a procedure for adduct pattern simplification. *Carcinogenesis,* **15,** 877–882.
12. Ishii, Y., Suzuki, Y., Hibi, D., Jin, M., Fukuhara, K., Umemura, T. and Nishikawa, A (2011). Detection and quantification of specific DNA adducts by liquid chromatography–tandem mass spectrometry in the livers of rats given estragole at the carcinogenic dose. *Chem. Res. Toxicol.,* **24,** 532–541.
13. Randerath, K., Haglund, R. E., Phillips, D. H. and Reddy, M. V. (1984) 32P-postlabelling analysis of DNA adducts formed in the livers of animals treated with safrole, estragole and other naturally-occurring alkenylbenzenes. I. Adult female CD-1 mice. *Carcinogenesis,* **5,** 1613–1622.
14. Phillips, D. H., Reddy, M. V. and Randerath, K. (1984) P-32 Post-labeling analysis of DNA adducts formed in the livers of animals treated with safrole, estragole and other naturally-occurring alkenylbenzenes. 2. Newborn male B6c3f1 mice. *Carcinogenesis,* **5,** 1623–1628.
15. Paini, A., Punt, A., Viton, F., Scholz, G., Delatour, T., Marin-Kuan, M., Schilter, B., van Bladeren, P. J. and Rietjens, I. M. C. M. (2010) A physiologically based biodynamic (PBBD) model for estragole DNA binding in rat liver based on in vitro kinetic data and estragole DNA adduct formation in primary hepatocytes. *Toxicol. Appl. Pharmacol.* **245,** 57–66.
16. Punt, A., Freidig, A. P., Delatour, T., Scholz, G., Schilter, B., Boersma, M. G., van Bladeren P. J. and Rietjens, I. M. C. M. (2008) A physiologically based biokinetic (PBBK) model for estragole bioactivation and detoxification in rat. *Toxicol. Appl. Pharmacol.,* **231,** 248–259.
17. Fisher, M. B., Campanale, K., Ackermann, B. L., VandenBranden, M. and Wrighton, S. A. (2000) In vitro glucuronidation using human liver microsomes and the pore-forming peptide alamethicin. *Drug Metab. Dispos.,* **28,** 560–566.
18. Lin, J. H. and Wong, B. K. (2002) Complexities of glucuronidation affecting in vitro in vivo extrapolation. *Curr. Drug Metab.,* **3,** 623–646.
19. Alhusainy, W. A. A. M., Paini, A., Punt, A. *et al.* (2010) Identification of nevadensin as an important herb-based constituent inhibiting estragole bioactivation and physiology-based biokinetic modeling of its possible in vivo effect. *Toxicol. Appl. Pharmacol.,* **245**, 179–190.
20. Manning, C. C., Schlosser, P. M. and Tran, H. T. (2010) A multicompartment liver-based pharmacokinetic model for benzene and its metabolites in mice. *Bull. Math. Biol.,* **72,** 507–540.
21. Jeurissen, S. M. F., Punt, A., Boersma, M. G., Bogaards, J. J., Fiamegos, Y. C., Schilter, B., van Bladeren, P. J., Cnubben, N. H. P. and Rietjens, I. M. C. M. (2007) Human cytochrome P450 enzyme specificity for the bioactivation of estragole and related alkenylbenzenes. *Chem. Res. Toxicol.,* **20,** 798–806.
22. Martignoni, M., Groothuis, G. M. M. and de Kanter, R. (2006) Species differences between mouse, rat, dog, monkey and human CYP-mediated drug metabolism, inhibition and induction. *Expert Opin. Drug Metabol. Toxicol.,* **2,** 875–894.
23. Oinonen, T. and Lindros, K. O. (1998) Zonation of hepatic cytochrome P-450 expression and regulation. *Biochem. J.,* **329,** 17–35.
24. Lindros, K. O. (1997) Zonation of cytochrome P-450 expression, drug metabolism and toxicity in liver. *Gen. Pharmac.,* **28,** 191–196.
25. Ullrich, D., Fischer, G., Katz, N. and Bock, K. W. (1984) Intralobular distribution of UDP-glucuronosyltransferase in livers from untreated, 3-methylcholanthrene- and phenobarbital-treated rats. *Chem. Biol. Interact.,* **48,** 181–190.
26. Chowdhury, J. R., Novikoff, P. M., Chowdhury, N. R. and Novikoff, A. B. (1985) Distribution of UDPglucuronosyltransferase in rat tissue. *Proc. Natl. Acad. Sci. U S A,* **82,** 2990–2994.

27. Delatour, T., Mally, A., Richoz, J. *et al.* (2008) Absence of 2'-deoxyguanosine-carbon 8-bound ochratoxin A adduct in rat kidney DNA monitored by isotope dilution LC-MS/MS. *Mol. Nutr. Food Res.,* **52,** 472–482.
28. Zeller, A., Horst, K. and Rychlik, M. (2009) Study of the metabolism of estragole in humans consuming fennel tea. *Chem. Res. Toxicol.,* **22,** 1929–1931.
29. Rietjens, I. M. C. M., Boersma, M. G. Zaleska, M. and Punt, A. (2008) Differences in simulated liver concentrations of toxic coumarin metabolites in rats and different human populations evaluated through physiologically based biokinetic (PBBK) modeling. *Toxicol. Vitro,* **22,** 1890–1901.
30. Rietjens, I. M. C. M., Louisse, J. and Punt, A. (2011) Tutorial on physiologically based kinetic modeling in molecular nutrition and food research. *Mol. Nutr. Food Res.,* **55,** 941–956.
31. Gyorffy, E., Anna, L., Kovács, K., Rudnai, P. and Schoket, B. (2008) Correlation between biomarkers of human exposure to genotoxins with focus on carcinogen-DNA adducts. *Mutagenesis,* **23,** 1–18.
32. EU-SCF (Scientific Committee on Food) (2001) Opinion of the scientific committee on food on estragole (1-allyl-4-methoxybenzene), http://ec.europa.eu/food/fs/sc/scf/out104_en.pdf.
33. Williams, G. M. (2008) Application of mode-of-action consideration in human cancer risk assessment. *Toxicol. Lett.,* **180,** 75–80.